A Carbohydrate Recognition–Based Drug Delivery and Controlled Release System using Intraperitoneal Macrophages as a Cellular Vehicle

Yuzuru Ikehara,[1] Toru Niwa,[1] Le Biao,[3] Sanae Kabata Ikehara,[1,2] Norifumi Ohashi,[1] Takeshi Kobayashi,[4] Yoshitaka Shimizu,[3] Naoya Kojima,[3] and Hayao Nakanishi[1]

[1]Division of Oncological Pathology, Aichi Cancer Center Research Institute; [2]Department of Epidemiology, Nagoya University Graduate School of Medicine, Nagoya, Japan; [3]Department of Applied Biochemistry and The Institute of Glycotechnology, Tokai University, Kanagawa, Japan; and [4]Department of Biological Chemistry, College of Bioscience and Biotechnology, Chubu University, Kasugai-shi, Japan

Abstract

The lymphoid tissue in the omentum, at the so-called milky spots, is known as an initial place for disseminated cancer cells to develop into solid tumors. In the present study, i.p. macrophages significantly took up oligomannose-coated liposomes (OMLs) that were injected into the peritoneal cavity, and then gradually accumulated in the omentum and the other lymphoid tissues within 24 hours of i.p. injection of OMLs. When 5-fluorouracil (5-FU) was encapsulated in the OMLs, >60% of administered 5-FU accumulated in the omentum. Treatment of macrophages at 39°C for 30 minutes led to the release of 5-FU from the macrophages, suggesting that controlled release from macrophages could be achieved by mild hyperthermia. We encased magnetic nanoparticles, which are known to convert electromagnetic energy to heat in the OMLs to achieve *in vivo* hyperthermia at the site. Using this system in a mouse i.p. metastasis model, we successfully controlled tumor development by coadministration of OML-encased 5-FU and OML-encased magnetic nanoparticles, followed by treatment with an alternating magnetic field. No apparent reduction was seen in tumor growth with the administration of OML-encased magnetic nanoparticles or OML-encased 5-FU alone. Thus, we have established the use of i.p. macrophages as a novel drug delivery system for the control of cancer metastatic to milky spots. (Cancer Res 2006; 66(17): 8740-8)

Introduction

Tumor progression into the peritoneal cavity indicates an unfavorable prognosis, with death resulting from peritonitis carcinomatosa (1). Gastric adenocarcinoma is a representative tumor in which i.p. dissemination predicts the noncurative recurrence, even in the early stages of the disease (2–4). Indeed, the identification or monitoring of dissemination in intraoperative peritoneal washings provides valuable prognostic information regarding whether i.p. recurrence will occur in the future (2, 4, 5).

Another characteristic feature of i.p. dissemination is that the subsequent solid tumor formation often occurs in the omentum (1). The omentum seems to be a central site where many types of disseminated tumor cells attach to make solid tumor (6). Viable disseminated gastric cancer cells have been detected in the omentum rather than in peritoneal washes (7), and the disseminated ovarian adenocarcinoma preferentially develops overt metastatic foci in the omentum (8). Omentectomy is widely done to reduce the risk of recurrence and to improve survival (9, 10). In addition, in a series of experimental studies, the omentum seemed to act as an initial implantation site for malignant cells (8, 11–14).

There are areas of aggregated inflammatory cells in the omentum (15), the so-called milky spots, and these sites seem to facilitate the adhesion and invasion of cancer cells. These possibly serve as active sites for the clearance of tumor cells from the peritoneal cavity. As inflammation has long been suspected to stimulate tumor growth (16–20), the interaction of tumor cells with such immune cells might support the formation of cancer metastases and solid tumors. In a series of recent molecular biological studies, nuclear factor-κB activation has been shown to play a pivotal role in these supportive functions (19, 20).

Although much progress has been made in the development and administration of chemotherapeutic drugs, surgery remains the curative treatment for digestive tract cancer. The most probable reason is that intra-abdominal tumor cells are not exposed to sufficient concentrations of anticancer drugs. To obviate this problem, the administration of chemotherapeutic agents into the peritoneal cavity using liposome-encapsulated drugs and the use of systems targeting tumor cells (21, 22) have been used in place of general methods, such as systemic i.v. chemotherapy, to concentrate the drugs in the tumor cells and metastatic foci (23, 24). However, the promising observations in these studies have not yet been translated into successful clinical therapies (1).

Another approach used to concentrate drugs at the required sites is the injection into the peritoneal cavity of mitomycin bound to activated carbon particles, leading to an expected accumulation in the milky spots. Although the results from two randomized trials were controversial (25, 26) and the effect of i.p. adjuvant therapy has not yet been established (27), this approach seems to be promising (21). The systemic administration of IFN-β failed to exert effects *in vivo* due to insufficient drug levels at the tumor site. In contrast, administration of human IFN-β via mesenchymal stem cells, which worked as targeted-delivery vehicles to the microenvironment of the solid tumor, reportedly succeeded in controlling metastatic tumor growth (28–30).

There are numerous macrophages in the milky spots in the omentum, and increased numbers of these spots are induced by various stimuli and cancer metastasis (31, 32). In addition, macrophages are professional phagocytes that can take up foreign particles, such as liposomes. Based on these characteristics, macrophages have been proposed as a cellular vehicle for targeting

Requests for reprints: Naoya Kojima, Department of Applied Biochemistry, Tokai University, 1117 Kitakaname, Hiratsuka-shi, Kanagawa 259-1292, Japan. Phone: 81-463-58-1211; Fax: 81-463-50-2012; E-mail: naoyaki@keyaki.cc.u-tokai.ac.jp.

doi:10.1158/0008-5472.CAN-06-0470

tumor tissue if the drugs and/or genes are efficiently and specifically delivered to the macrophages (33, 34). However, definitive evidence for the utility of macrophages as vehicles has yet to be provided and awaits detailed *in vivo* trafficking studies.

As macrophages express carbohydrate receptors, such as macrophage-mannose-receptor (CD206), to recognize invaded pathogens, we hypothesized that the receptors are potential targets for the specific delivery to the cells. We thus synthesized neoglycolipids consisting of oligosaccharides and dipalmitoylphosphatidylethanolamine (DPPE), and examined the applications of these materials. Our results showed that liposomes coated with a neoglycolipid consisting of DPPE and mannotriose (Man3) were most efficiently incorporated into i.p. macrophages among liposomes coated with neoglycolipid with other types of oligosaccharides. These findings led us to the idea that the oligomannose-coated liposome (OML) may be used as a platform for a new drug delivery method to successfully accumulate anticancer drug at the i.p. metastatic sites via i.p. macrophages. In this study, we developed techniques for targeting the accumulation of anticancer drugs to milky spots using i.p. macrophages and anticancer drugs encased in OMLs. In addition, we established methods for controlled release of the drugs from macrophages at the desired site. These techniques for active delivery and controlled release of anticancer drugs effectively suppressed growth of cancer cells in the omentum in a model of disseminated cancer, suggesting that the new drug delivery and controlled release method can be exploited therapeutically.

Materials and Methods

Mice. Female C57BL6 (B6) mice, 7 to 10 weeks old, and male athymic mice of the KSN strain were obtained from Charles River Japan, Inc. (Kanagawa, Japan), and the Shizuoka Laboratory Animal Center (Hamamatsu, Japan), respectively. The B6 mice were kept under standard housing conditions, and the KSN athymic mice were maintained under specific pathogen-free conditions. All animal experiments were done under the experimental protocol approved by the Ethics Review Committee for Animal Experimentation of the Aichi Cancer Center.

Cell lines. The MKN28 and the GCIY human gastric cancer cell lines were obtained from the RIKEN cell bank. MKN28 and GCIY cells with stable expression of green fluorescent protein (GFP; MKN28-EGFP and GCIY-EGFP) were established in our laboratory, as previously described (35). MKN28-EGFP and GCIY-EGFP cells were maintained in DMEM (Nissui Pharmaceutical Co., Ltd., Tokyo, Japan) containing 10% fetal bovine serum (Life Technologies, Grand Island, NY) with 300 μg/mL G418 (Wako, Osaka, Japan) in a humidified 5% CO_2 incubator at 37°C.

Neoglycolipid and liposome preparation. Dipalmitoylphosphatidylcholine (DPPC), cholesterol, and DPPE were purchased from Sigma-Aldrich (St. Louis, MO). Mannotriose [Man3: Manα1-6(Manα1-3)Man], mannopenntaose [Man5: Manα1-6(Manα1-3)Manα1-6(Manα1-3)Man], biantenary *N*-linked core pentasaccharide [GlcNAcβ1-2Manα1-6(GlcNAcβ1-2Manα1-3)Man], LNT [Galβ1,3GlcNAcβ1,3Galβ1,4Glc], and FLNT [Fucα1,2Galβ1,3GlcNAcβ1,3Galβ1,4Glc] were from Funakoshi, Co., Ltd. (Tokyo, Japan). The neoglycolipids were prepared by conjugation of these oligosaccharides with DPPE by reductive amination as described previously (36). In brief, 20 μmol of the oligosaccharide and 70 μmol DPPE were dissolved in 5 mL chloroform/methanol/water (10:10:1, v/v/v). The mixture was sonicated (10 minutes) in a sonic bath and heated at 37°C for 2 hours in a reaction vial sealed with a Teflon-lined cap. Then, 300 μmol sodium cyanoborohydride dissolved in methanol (1 mL) was added, and the reaction mixture was kept at 80°C for 5 hours. After removing the solvent under a stream of N_2, the residues were suspended in 10 mL chloroform/methanol/water (4:50:50, v/v/v), and applied on a C18 column (Bond Elute, MEGA BE-C18, Varian, Harbor City, CA) equilibrated with the same solvent. After the column was washed with 50 mL chloroform/methanol/water (4:50:50, v/v/v), the clued lipids were eluted from the column with 30 mL chloroform/methanol/water (10:10:3, v/v/v). Purification of the neoglycolipid from the clued lipid sample was done by high-performance liquid chromatography (HPLC) on a silica column (Wakosil 5SIL-120, 0.75 × 30 cm, Wako Pure Chemical, Tokyo, Japan) with a linear gradient of chloroform/methanol/water (65:30:5) and chloroform/methanol/water (50:55:18). The structure and the purity of the neoglycolipid were confirmed by high-performance TLC and matrix-assisted laser desorption/ionization–time-of-flight mass spectrometry (Auto FLEX, Bruker Daltonics, Bremen, Germany). The purified neoglycolipid was quantified by determination of phosphate and hexose.

Liposomes containing the neoglycolipids were prepared as described previously, with modification. Briefly, a chloroform/methanol (2:1, v/v) solution containing 1.5 μmol DPPC and 1.5 μmol cholesterol was placed in a conical flask and dried by rotary evaporation. Subsequently, 2 mL ethanol containing 0.15 μmol of respective neoglycolipid was added to the flask and evaporated to prepare a lipid film containing neoglycolipids. The multilamellar vesicles were generated with either 200 μL 5-fluorouracil (5-FU, Kyowa Co., Tokyo, Japan), FITC-labeled bovine serum albumin (BSA, 5.0 mg/mL, Sigma-Aldrich, Saint Louis, MO), TRITC-labeled BSA (5.0 mg/mL, Sigma-Aldrich), or PBS in the dried lipid film by intense vortex dispersion. The multilamellar vesicles were extruded 10 times through a 1 μm pore polycarbonate membrane (Nucleopore, Pleasanton, CA). For fluorescent labeling of the lipid bilayer in the OMLs, a lipid film containing 0.15 μmol NBD-DPPE was used. The amount of 5-FU encased in the liposomes was determined as described below, and was adjusted to 60.0 ± 1.2 μg/mg cholesterol.

For preparation of liposomes encasing magnetic nanoparticles, magnetite nanoparticles (Fe_3O_4; average particle size 10 nm) were prepared as described previously (37). Briefly, $NaNO_2$ and Fe_2SO_4 were mixed well to precipitate Fe_3O_4 magnetite nanoparticles, which were spun down and washed with distilled water. The nanoparticles were then coated with lauric acid by mixing with an excess volume of lauric acid at 90°C so as to generate single particles. Free lauric acid was removed by dialysis of the particles against distilled water. The lauric acid–treated nanoparticles were transferred onto a neoglycolipid-containing lipid film, and then mixed well to generate multilamellar vesicles containing Fe_3O_4 magnetic nanoparticles. The amount of magnetite particles encased in the liposome was determined by the concentration of Fe^{2+} and was adjusted to 1.87 ± 0.23 mg/mg of cholesterol.

Flow cytometry, fluorescence microscopy, and immunohistochemistry. The surface expression of F4/80 on peritoneal cells was routinely evaluated by fluorescence-activated cell sorting (FACS; FACSCalibur, BD Science, San Diego, CA) using direct staining with immunofluorescent antibody as previously described (38). One hour after injection of either OMLs or bare liposomes encasing FITC-labeled BSA into the peritoneal cavity of mice, peritoneal cells were recovered with 5 mL cold PBS. Peritoneal cells were incubated on ice for 30 minutes with red-phycoerythrin–conjugated anti-F4/80 antibody after blocking with mouse BD Fc Block (BD Science). For confocal microscopy, stained peritoneal cells were mounted on glass slides using ProLong Gold antifade reagent (Molecular Probes, Eugene, OR) to reduce photobleaching during observation.

For immunohistochemical detection of FITC-conjugated BSA that was taken by macrophages to the omentum, sections were incubated with peroxidase-labeled polyclonal anti-FITC antibody (Roche Diagnostic, Co., Tokyo, Japan) overnight at 4°C. The antibody reaction was visualized with a diaminobenzidine/H_2O_2 solution.

Model of gastric cancer i.p. metastasis. MKN28-EGFP and GCIY-EGFP cells were used to generate experimental metastases in the peritoneal cavities of athymic mice as described previously (35). Cells (3×10^6 in 0.4 mL) were then injected into the peritoneal cavities of athymic mice. About 6 hours after injection, metastatic foci in the omentum were visualized through the abdominal wall under a dissection microscope (SZ4-GFP, Olympus, Tokyo, Japan) using a fluorescence imaging system (FIS) with excitation light (450-490 nm) from an LG-PS halogen source (Olympus) and a cutoff filter (emission from 530 nm). For the detection of

macrophages that took up liposomes encasing TRITC-labeled BSA, we used excitation light (longer than 540 nm) generated using a long-pass filter (Kodak, Rochester, NY) and an LG-PS halogen source.

Determination of 5-FU. To determine the amount of 5-FU encased in the liposomes, the liposomes were treated with a 1% SDS solution, and subjected to HPLC using an octadecyl silane column (Mightysil RP-18 GP, 4.6 × 250 mm, Kanto Kagaku, Tokyo, Japan) equilibrated with 1% methanol, and eluted under isocratic conditions. For determination of 5-FU in macrophages, the peritoneal cells were seeded into the wells of six-well plates and cultured for 4 hours to remove nonadherent cells. The adherent cells (macrophages) were lysed with 0.5 mL of 0.1% SDS containing 1% trichloroacetic acid, and subjected to HPLC to determine 5-FU. For the determination of the amount in omenta, they were lysed with 0.5 mL of 0.1% SDS containing 1% trichloroacetic acid. For the determination in culture medium, recovered medium were lyophilized and dissolved in 0.5 mL of 0.1% SDS containing 1% trichloroacetic acid, incubated at 100°C for 10 minutes.

Therapeutic procedures used in the peritoneal metastasis model. Metastatic foci in the omentum were observed through the abdominal wall using FIS at 6 hours after injection of either MKN28-EGFP or GCIY-EGFP cells (3×10^6 in 0.4 mL) into the peritoneal cavities of athymic mice. Twenty-four hours after the injection of the cells into the peritoneal cavities of athymic mice, anticancer agents or OML-encased anticancer agents were injected. The effect of chemotherapy was evaluated as described previously (35). If necessary, OMLs encasing magnetic particles were coinjected with OMLs encasing anticancer agents. On the next day, *in vivo* hyperthermia was produced by means of an alternating magnetic field. One week after the treatment, mice were killed and GFP-tagged tumor cells were visualized as described above. Then, the tumor cells were excised, based on the locations of fluorescent signals under the dissection microscope, and the tumor weight was measured. The alternating magnetic field was created using a horizontal coil (inner diameter 5 cm, length 8 cm) with a transistor inverter (Dai-ichi High Frequency, Tokyo, Japan). Anesthetized mice were laid in the center of the magnetic field. The magnetic field frequency and intensity were 118 kHz and 10 kA/m (125 Oe), respectively.

Results

Peritoneal macrophages efficiently took up OMLs. To know whether the surface coating with neoglycolipids makes for more efficient liposome uptake by macrophages, the fluorescently labeled BSA-encased liposomes coated with or without a series of neoglycolipids were prepared and injected into the peritoneal cavities of B6 mice. One hour after the injection, the fluorescent signals from encapsulated FITC-BSA in peritoneal cells were determined for evaluation of the liposome incorporation by FACS (Fig. 1*A*). The representative results indicated that the liposomes coated with Man3-DPPE were incorporated into peritoneal cells most efficiently among the tested liposomes coated with neolygolipids with other types of oligosaccharides. Our estimation revealed that the liposomes coated with Man5-DPPE or Man3-DPPE were the best compounds for macrophage uptake. The liposomes coated with Man3-DPPE was slightly better than Man5-DPPE (means of fluorescence intensity was 544.5 on M3 and 436.6 on M5, data not shown), although the difference was not statistically significant. The liposome coated with Man3-DPPE was thus used in the present study in light of its higher incorporation by macrophage. Most of the resident macrophages (over 70% of $F4/80^+$ cells) presented an intense signal from the fluorescently labeled BSA in the OMLs due to the uptake. In contrast, only 5.5% of $F4/80^+$ cells exhibited a positive but weak signal from bare liposomes (Fig. 1*B*). The uptake was confirmed by visualization using a confocal microscope. As shown in Fig. 1*B*, TRITC-BSA (red) was detected in the cytoplasm, whereas FITC-F4/80 antibody (green) was on the cell surface of cells from OML-injected mice. When the liposome membrane was labeled with NBD-labeled DPPE (NBD-DPPE), the encased TRITC-BSA (red) and liposome (green) signals were completely colocalized in the cytoplasm of the macrophages (data not shown). These results suggested that the materials encased in the OMLs were efficiently incorporated into peritoneal macrophages as liposome particles. Time course analysis showed that the incorporated OML signals reached a plateau within 30 minutes. The uptake efficiency was the same for 1 hour and then gradually decreased over the following 12 hours (data not shown).

We then traced the fluorescent signals to determine the homing site of the cells that had incorporated the liposomes. To detect the signals using an FIS, OMLs encasing FITC-BSA were prepared and injected into the peritoneal cavities of mice. Twenty-four hours after the OML injection, a bright fluorescent signal was seen in the omentum (Fig. 1*C*) and detected up to 60 hours after the injection. The signals from OMLs in the homing cells were immunohistochemically confirmed using a specific antibody against FITC-labeled BSA. FITC-BSA was stored in the cytoplasm of phagocytic cells at the milky spots in the omentum (Fig. 1*C*) and peritoneum (data not shown), whereas no apparent accumulation was seen in the mice that received bare liposomes (Fig. 1*D*). To determine whether OMLs accumulated in the omentum, we traced the FITC-conjugated BSA that was encased in the OMLs by using FIS. The results in Fig. 2 show that the fluorescent signals in the omentum increased gradually and reached a plateau within 24 hours of injection. Taken together, these results suggest that the macrophages homed to the milky spots after the uptake of OMLs.

Macrophages accumulate in the omentum, a hotspot for i.p. metastasis. Next, we wished to determine whether the place at which accumulation of OMLs occurred was the same as that at which cancer metastasis frequently arises. As recent progress in GFP-tagging techniques has made it easy to trace cancer progression under FIS in animal models, we have established and developed a gastric cancer model of i.p. dissemination using MKN28 and GCIY cells transduced to stably express GFP. Six hours after the injection of GFP-tagged cancer cells into the peritoneal cavities of athymic mice, the cells gathered at the milky spots in the omentum, as previously shown (35). Established metastases were confirmed by the fluorescence signals from GFP observed through the abdominal wall under FIS. Using this system, we investigated whether macrophages taking up OMLs accumulated around metastases in the omentum. The results in Fig. 3 clearly show that MKN28-EGFP cells vegetate in the omentum, and that macrophages accumulate in the metastatic foci (Fig. 3*B*) in the specimens excised from between the spleen and omentum. The merged image in Fig. 3*B* indicates colocalization of the metastases and OML deposits. The same results were obtained when GCIY-EGFP cells were used (data not shown). These results suggest the possibility of using OMLs as a new tool for drug delivery targeted to metastatic foci in the peritoneal cavity.

Targeted accumulation and controlled release of 5-FU at i.p. metastatic sites. We next sought to determine whether the accumulation of OMLs containing anticancer reagent was effective against metastatic foci in the omentum. 5-FU is commonly used in the treatment of gastric cancer due to its active chemotherapeutic effects of inhibiting growth and initiating apoptosis. To examine how much 5-FU encased in OML was accumulated in the omentum by macrophage delivery,

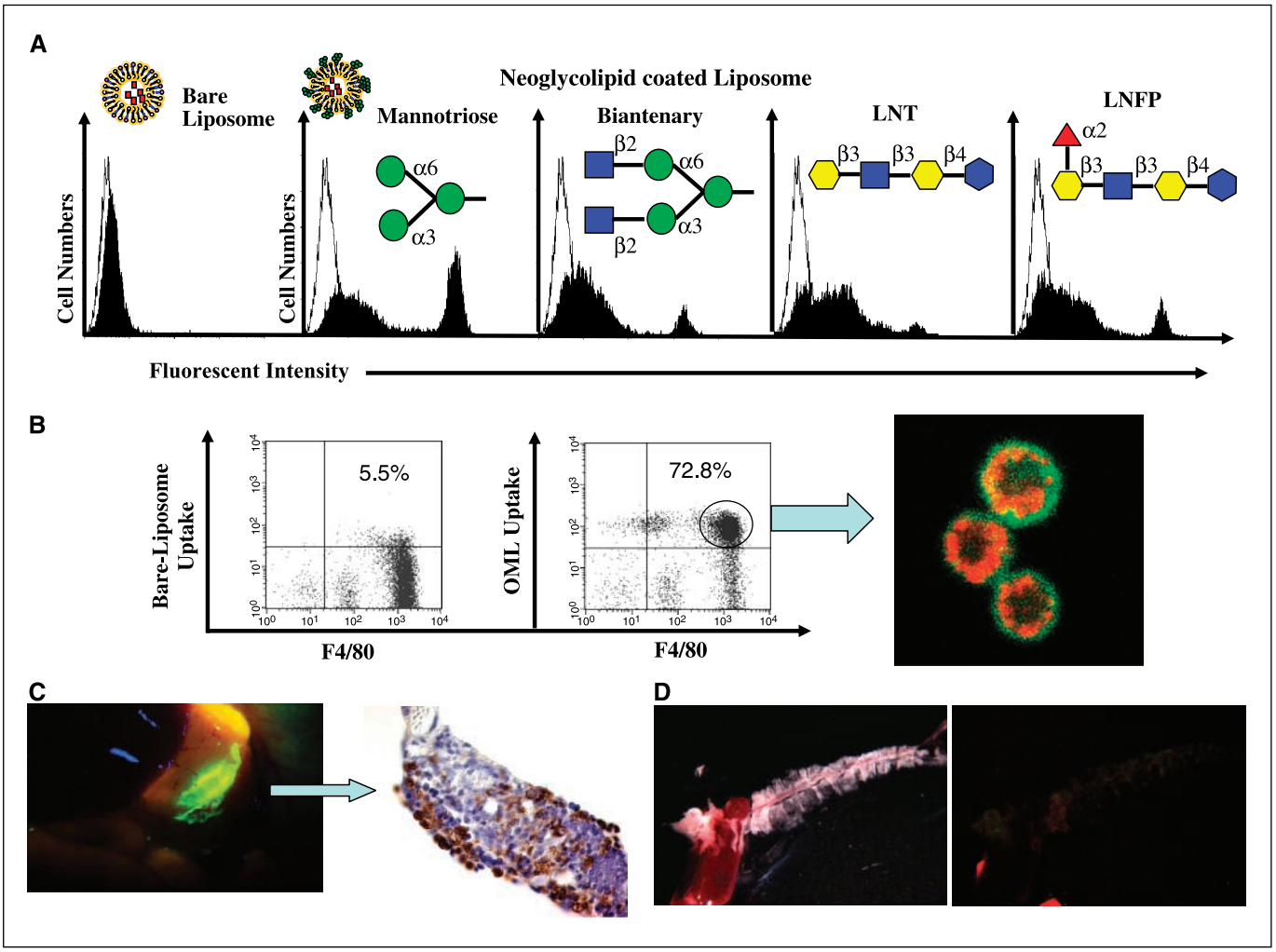

Figure 1. With intensive OML uptake by peritoneal cells, the omentum serves as a major homing site for cells incorporating the liposome. Multilamellar vesicles were generated with fluorescent-labeled BSA. *A,* liposomes with or without the neoglycolipid were injected into the peritoneal cavities of mice, and peritoneal cells were evaluated for uptake efficiency. Carbohydrate structures were shown according to the symbol nomenclature by Consortium for Functional Glycomics (http://www.functionalglycomics.org). *B,* liposomes with or without the mannotriose were injected into the peritoneal cavities of mice, and the macrophages detected by FITC-labeled anti-F4/80 antibody were evaluated for liposomes uptake. Bare liposomes were taken up by 5.5% of F4/80$^+$ macrophage cells, whereas OMLs were detected in 72.8% of the F4/80$^+$ cells. Gated cells were analyzed by confocal microscopy. FITC-labeled anti-F4/80 antibody reacted on the cell surface (*green*), whereas OMLs containing TRITC-labeled BSA were detected in the cytoplasm of F4/80$^+$ cells. *C,* FITC-BSA encased in OMLs was prepared and injected into the peritoneal cavities of mice. Twenty-four hours after the OML injection, a bright fluorescent signal was detected in the omentum using FIS. By immunohistochemical analysis with anti-FITC monoclonal antibody, FITC-BSA (*brown signals*) was detected in larger foamy cells but not in small round cells. Brown signals located in the cytoplasm of the larger cells. Further immunohistochemical analysis using specific monoclonal antibodies revealed that small round cells were B or T lymphocytes, and that the large cells were macrophages (data not shown). *D,* bright field (*left*) and FIS image (*right*) show no apparent accumulation in the mice that received bare liposome.

injections and evaluations were done as described in Materials and Methods. The representative result shown in Fig. 4*A* shows that ~60% of the injected 5-FU (up to 30 μg) accumulated in the omentum, and it persisted for as long as FITC-BSA was delivered by macrophages, which in preliminary experiments was detected in macrophages 60 hours after injection. Furthermore, although the accumulation of 5-FU seems to be sufficient to control cancer growth in the omentum, the administration of OMLs encasing 5-FU into the peritoneal cavity was not able to control cancer growth (data not shown). Consequently, we tried to apply the controlled release of the contents of the macrophages, so to expose tumor cells at the foci.

One of the promising methods of controlled release noted in earlier studies was mild warming, which could force rabbit peritoneal macrophages to release the intracellular components (39). Peritoneal cells recovered 1 hour after the injection of 5-FU encased in OMLs were incubated for 30 minutes at various temperatures. After a second incubation for 24 hours at 37°C, the amounts of 5-FU in the culture medium and cells were determined. As shown in Fig. 4*B*, hyperthermia in excess of 40°C led to the release of 5-FU into the culture medium from peritoneal cells. Although cell viability significantly decreased with 43°C incubation, 40°C apparently did not harm the cells (data not shown). Therefore, hyperthermia (39°C or 40°C for 30 minutes) could release 5-FU into the omentum after transport by macrophages (Fig. 4*C*), and mild warming is thus a promising procedure for the controlled release of the delivered 5-FU.

Use of OMLs encasing magnetic nanoparticles to produce hyperthermia in the omentum. To establish a controlled release method using mild heat stimulation, we used magnetite nanoparticles,

which have been widely used in hyperthermal treatment of a variety of tumors (40–42). As they mediate the change of electromagnetic energy to heat (43), these magnetite nanoparticles would specifically heat macrophages producing intracellular hyperthermia if the nanoparticles had been delivered appropriately. When OML-encased magnetite particles were injected into the peritoneal cavity, up to 160 μg of magnetite accumulated in the omentum 24 hours after the injection (Fig. 5*A*). The distribution of OML-encased magnetite particles was restricted to the omentum (Fig. 5*B*), where macrophages stored the particles (data not shown). In contrast, bare liposomes encasing magnetite were deposited exclusively in the liver (Fig. 5*B*). These results suggest that OML-encased magnetite can act as an inducer for heat stimulation to release materials carried by macrophages.

Novel drug delivery and controlled release system reduced tumor growth at metastatic foci. To allow use of *in vivo* hyperthermia to release anticancer drugs from macrophages at metastatic foci, the injected amounts of OML-encased 5-FU and OML-encased magnetite were optimized according to their accumulation efficiencies in the omentum. From a series of experiments, we found that coinjection of 14 μg 5-FU in OMLs (230 μg of cholesterol) and 60 μg magnetite in OMLs (30 μg of cholesterol) showed a suitable accumulation efficiency. Based on this condition, we evaluated whether application of the targeted delivery and controlled release technique to anticancer agents could control the growth of tumor cells at metastatic foci. Mixtures of 14 μg 5-FU in OMLs and 60 μg magnetite in OMLs, PBS in OML and 60 μg magnetite in OML, or 14 μg of 5-FU, were injected into the peritoneal cavities of athymic mice 24 hours after injection of MKN28-EGFP cells (3×10^6). On the next day, the mice were exposed to an alternating magnetic field for 30 minutes. After the treatment, MKN28-EGFP growth in the i.p. metastasis was traced every day with the GFP signals through the abdominal wall by FIS. As it was difficult to observe the signals in mice treated with mixtures of 14 μg of 5-FU in OMLs and 60 μg of magnetite in OMLs 1 week after the treatment, all mice were sacrificed and GFP-tagged tumor cells were visualized as described above. Then, the tumor cells were excised, based on the locations of fluorescent signals under the dissection microscope, and the tumor weight was measured.

As shown in the representative results in Fig. 6, the growth of i.p. disseminated MKN28-EGFP cells was significantly reduced when the mixture of 5-FU in OMLs and magnetite in OMLs was injected. In contrast, injection of the mixture of PBS in OML and magnetite in OML did not cause such an effect, suggesting that the effect of hyperthermia alone on the reduction of tumor cell growth is negligible in this system. In addition, a significant reduction in tumor growth was not observed following direct injection of a corresponding amount of 5-FU, as well as a 2,000-fold amount of 5-FU. These results strongly suggest that the described targeted delivery and controlled release of anticancer agents by combined use of OMLs and hyperthermia may be valuable for use in the control of i.p. metastatic malignancies.

Discussion

Here, we describe a new drug delivery method using the carbohydrate recognition by macrophages applied for a cellular vehicle in a drug delivery system so as to control tumor development at milky spots in the omentum, where solid tumors preferentially develop. The novel system uses two distinct technical approaches. The first approach was improvement of the direction of liposomes to macrophages, which was achieved by the

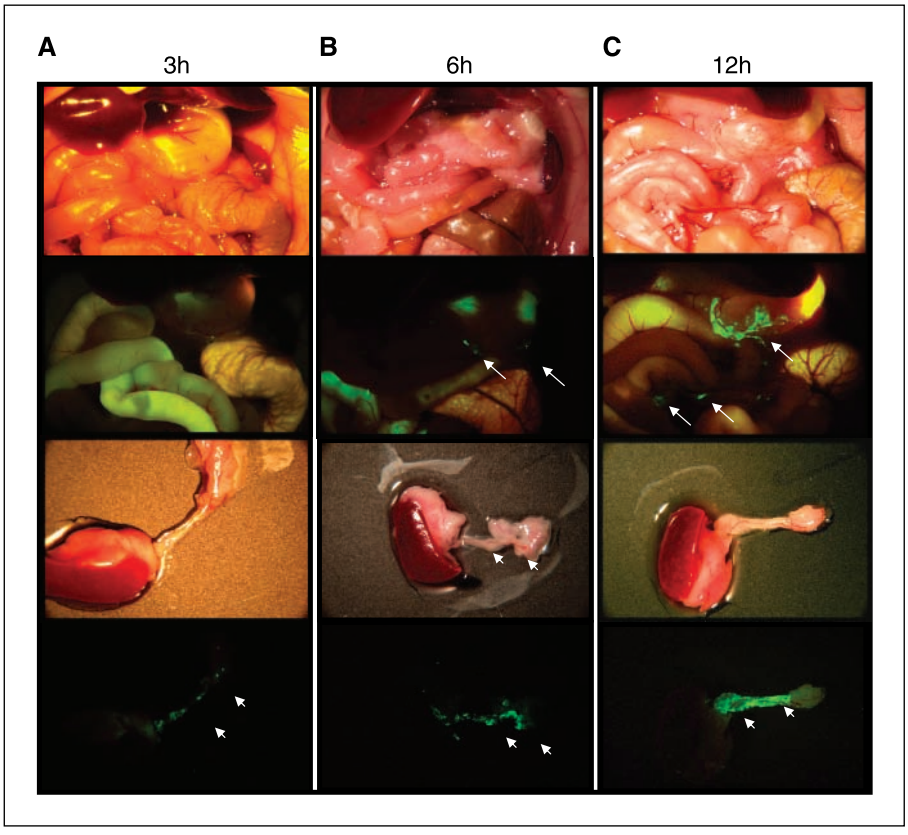

Figure 2. Injected OMLs gradually accumulated in the omentum. OMLs that were taken up by i.p. macrophages could be traced by the detection of FITC-conjugated BSA by FIS. *A* to *C,* images from a bright-field dissection microscope (*first and third from the top*) and from FIS (*second and fourth from the top*) at 3, 6, and 12 hours after the injection of OMLs. Fluorescent signals in the omentum (*arrow*) gradually increased and reached a plateau within 24 hours of injection (*second row from top*). The omentum was removed with the spleen (*third row*), and OML accumulation was evaluated. Small accumulations of OML were detected from 3 to 6 hours, whereas significant signals were detected in the omentum (*arrowhead*) 12 hours after the injection (*bottom row*).

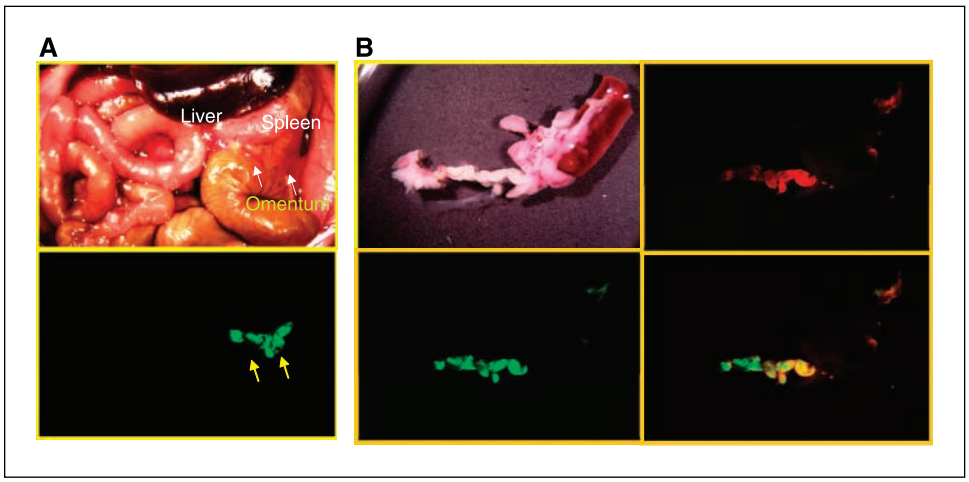

Figure 3. Liposomes accumulated at sites of cancer metastases. Six hours after injection of MKN28-EGFP cells into the peritoneal cavities of athymic mice, the cells gathered at the milky spots in the omentum, resulting in the establishment of metastases. The next day, OMLs encasing TRITC-labeled BSA were injected into the peritoneal cavities of mice. *A,* MKN28-EGFP cells vegetated in the omentum (*top, white arrows in the bright field*) and were detected by FIS as green fluorescent signals (*yellow arrows in bottom row*). *B,* the excised omentum (*left top*) showed OML accumulation (*right top; red signal*) and cancer metastases (*left bottom; green signal*). The yellow signal in the merged image indicates the colocalization of the metastases and OML accumulation (*right bottom*).

carbohydrate recognition by macrophages for a neoglycolipid with oligomannose residues. After injection of OMLs into the peritoneal cavity, macrophages specifically took them up within 1 hour, and most (~60%) of the liposome-encased materials stored in macrophages consequently appeared in the milky spots in the omentum within 24 hours. The second approach was to use the macrophage characteristic of releasing intracellular components when exposed to mild hyperthermia. To deliver *in vivo* hyperthermia to macrophages, we used OML-encased magnetic nanoparticles, which are known to convert electromagnetic energy to heat. We showed that the OML-encased magnetic nanoparticles accumulated in the omentum, and when OML-encased magnetic nanoparticles and OML-encased 5-FU were coinjected and hyperthermia was applied, tumor development in the omentum was significantly suppressed. Accordingly, this novel targeted delivery method should translate to effective control of i.p. metastasis, although the detailed mechanisms involving the uptake of liposomes and macrophage accumulation remain to be elucidated.

As the anticancer drugs in the liposome were delivered to tumor cells by macrophages, our approach is unique because of the indirect liposome delivery. To date, conventional liposome delivery methods have been used to deliver drugs directly and efficiently to tumor cells, and the liposomes have been coated with polyethyleneglycol, to prevent uptake by macrophages, and/or specific ligands, to improve accumulation in the cancer cells (22–24).

Of note is that our approach using a device to release anticancer drugs at the milky spots of the omentum is unprecedented. Previous studies used mitomycin bound to activated carbon particles and 5-FU microspheres to allow accumulation of the anticancer drug at the required site, and anticipated release of the drug in a passive manner according to the adsorption equilibria (25, 26). Consequently, this targeted delivery method consists of the application of successive cellular responses of macrophages in the processes of loading, delivery, and deposition of materials. Figuratively speaking, we used the macrophages as "cellular vehicles" and the OMLs as "microcargo" to deliver the drug to the omentum. Thus, our approach is conceptually different from previous drug delivery methods.

In the field of gene therapy, macrophages have been used as "cellular vehicles" to deliver genes to distant sites because of

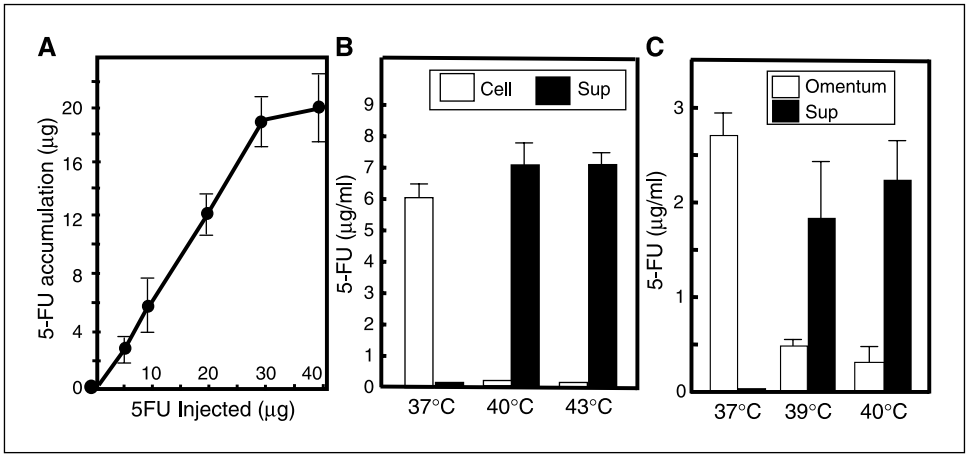

Figure 4. Macrophages carried OML-encased 5-FU to the omentum, which were released by mild heating. *A,* OMLs encasing 5-FU were injected into mouse peritoneal cavities, and omenta were recovered after 24 hours. Dissected omenta were lysed with 0.5 mL of 0.1% SDS containing 1% trichloroacetic acid, and samples were subjected to HPLC. The amount of accumulated 5-FU increased with increasing amounts of injected OMLs encasing 5-FU. *B,* macrophages recovered 1 hour after injection of OMLs containing 5-FU were incubated for 30 minutes at various temperatures. After a second incubation for 24 hours at 37°C, the amounts of 5-FU were determined as described in Materials and Methods. Hyperthermia at over 40°C led to 5-FU release into the culture medium from peritoneal cells. *C,* omentum was cut out from mice 24 hours after injection of OMLs containing 5-FU, which was subjected to hyperthermia in culture medium at 39°C or 40°C for 30 minutes. After a second incubation for 24 hours at 37°C, the 5-FU released from the omentum was determined.

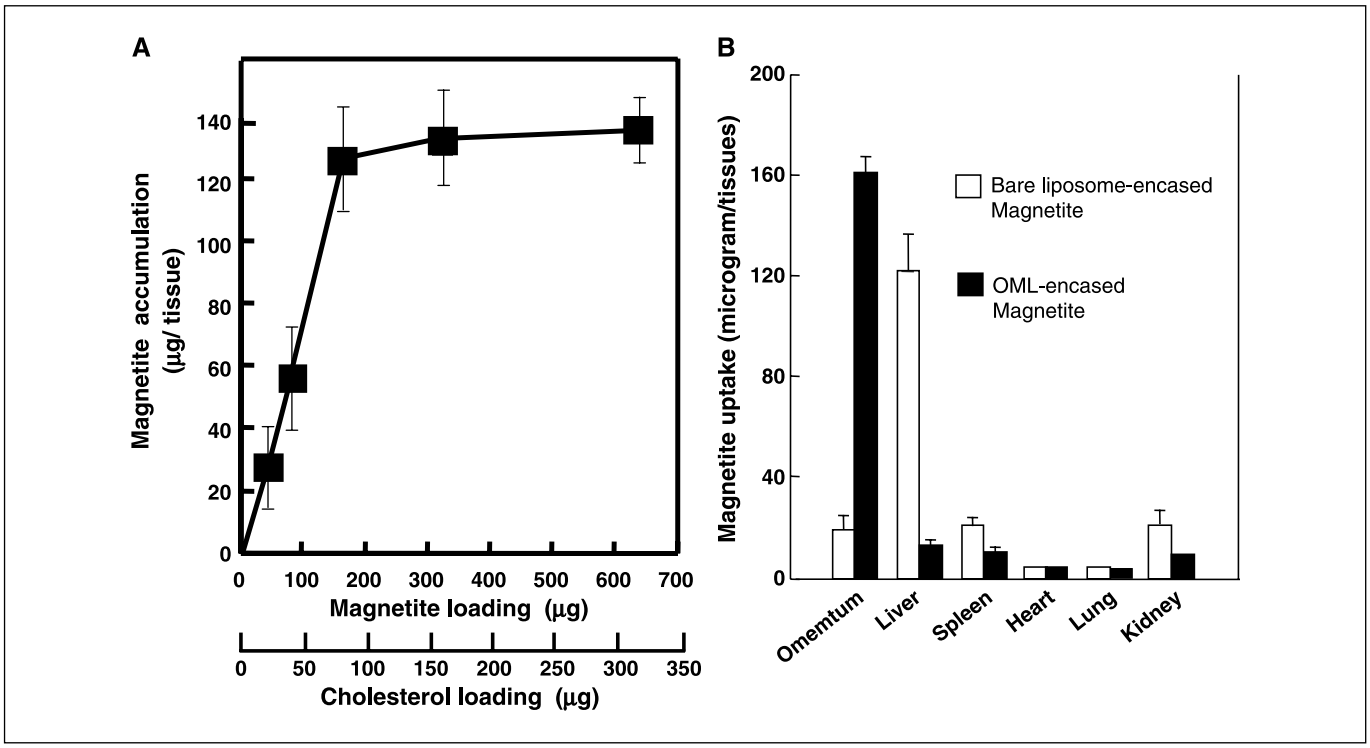

Figure 5. OML-coated magnetite particles were exclusively distributed to the omentum. Magnetic nanoparticles encased in liposomes (OMLs and bare liposome) were injected into the peritoneal cavities of athymic mice. One day after the injection, omenta, livers, spleens, hearts, lungs, and kidneys were recovered to determine the amount of accumulated magnetite. *A,* injection of increasing amounts of OML-coated magnetite particles resulted in accelerated accumulation in the omentum. *B,* magnetic nanoparticles encased in OMLs accumulated in the omentum, whereas bare liposomes distributed to the liver, spleen, and kidney.

their natural tendency to migrate to pathologic lesions (33, 34). Therefore, OMLs highly directed to macrophages can be potentially used as a platform for specific delivery by macrophages of not only anticancer drugs but also genes and other biological materials to treat the tumor stroma in cancer. The delivery of cytokines or cytokine genes, such as IFN-β, to newly migrating macrophages is a valuable potential application of this platform, because such treatment is expected to alter the macrophage phenotype from tumor-supporting to a more cytotoxic and antigen-presenting phenotype. Furthermore, our platform could be used for immunogene therapy, by way of establishing *ex vivo* gene transfer to macrophages and their reintroduction into the peritoneal cavity. Alternative investigations are required to substantiate whether this platform is valid for application to tumor-associated macrophages (TAMs) as well as common macrophages *in vivo*. The macrophages infiltrating into cancer tissue are known as TAMs, and they seem to support cancer growth due to their secretion of cytokines and growth factors (44).

Coincident accumulation around metastatic sites of macrophages that have taken up OMLs may pose a potential limitation to the use of this platform in practice because this accumulation is considered to increase the risk of creating a microenvironment favorable for cancer development (44). It has long been suspected that interactions between inflammatory cells and cancers promote cancer growth. Histologically, macrophages that accumulate around tumors are believed to be TAMs. Results from studies using mouse models have shown that secondary metastases are derived from newly generated milky spots that appear around the first metastatic spots (14). Therefore, the accumulation of foci of inflammatory cells would act as "soil" for the growth of cancer cells as "seed" (45). However, fewer and smaller residual tumor nodules in the treated mice were observed than in nontreated mice because of the maintenance of higher drug concentrations at the site of macrophage accumulation after the hyperthermia. In addition, we did not observe increased dissemination in the treated mice. These data suggest that the advantages of the treatment might overcome the risk of further cancer development due to accumulation of OML-loaded macrophages.

To achieve a better prognosis for patients with i.p. metastases and to improve the effectiveness and tolerability of cancer chemotherapy, the establishment of such efficient delivery systems is crucial. It is to this end that we have introduced an altogether new approach involving OMLs as a platform to control progression of such tumors. This new platform can be applied to therapeutic technologies, not only in malignant diseases but also in other diseases including immune diseases and atherosclerosis. In the future, molecularly targeted drugs, antibodies, decoy receptors, cytokines, and genes may be delivered by this novel technique.

Acknowledgments

Received 2/7/2006; revised 5/18/2006; accepted 7/3/2006.

Grant support: Industrial Technology Research Grant Program in 2004 from New Energy and Industrial Technology Development Organization of Japan, and a grant for Hi-tech research program from Tokai University.

The costs of publication of this article were defrayed in part by the payment of page charges. This article must therefore be hereby marked *advertisement* in accordance with 18 U.S.C. Section 1734 solely to indicate this fact.

We thank Dr. James C. Paulson (The Scripps Research Institute, La Jolla, CA) for scientific discussion in preparing the manuscript.

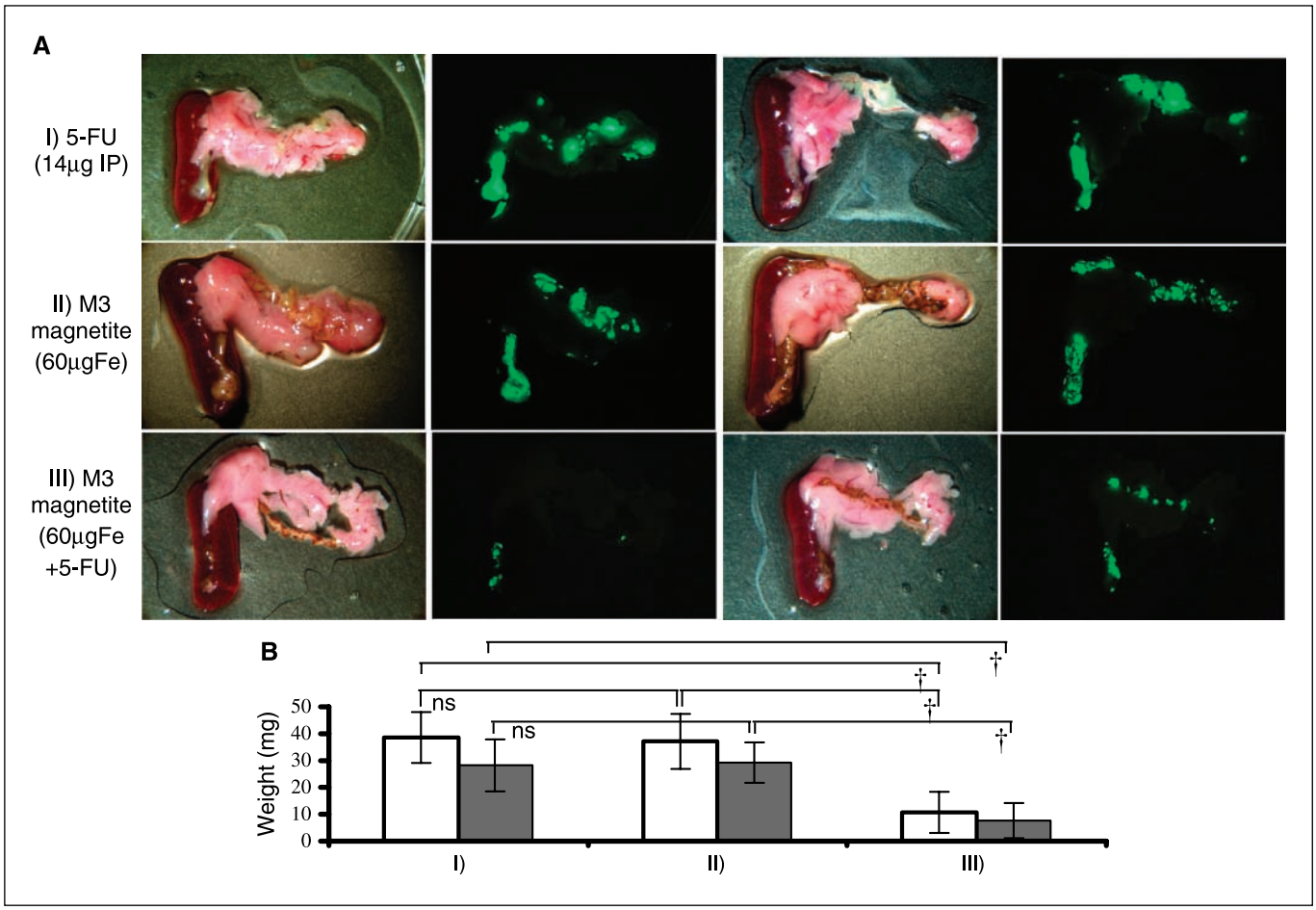

Figure 6. Cancer metastases were controlled by coinjection of OML-encased 5-FU and OML-coated magnetite. *A,* MKN28-EGFP cells (3×10^6 in 0.4 mL) were injected into the peritoneal cavities of athymic mice, and the metastatic foci in the omentum were confirmed through the abdominal wall by FIS. Mice were divided into three groups and injected into the peritoneal cavities with either (*I*) 14 μg 5-FU, (*II*) a mixture of PBS in OMLs and 60 μg of magnetite in OMLs, or (*III*) a mixture of 14 μg 5-FU in OMLs and 60 μg magnetite in OMLs 24 hours after inoculation of the cancer cells. On the next day, mice were exposed to an alternating magnetic field for 30 minutes. As shown in these representative results, peritoneal dissemination of MKN28-EGFP cells was significantly reduced when the mixture of 5-FU in OMLs and magnetite in OMLs was injected. In contrast, injection of the mixtures of PBS in OMLs and magnetite in OMLs did not produce such an effect. *B,* significant reduction of tumor growth was seen in total tumor (*open column*) and in the omentum (*gray column*) on group III (14 μg 5-FU in OMLs and 60 μg magnetite in OMLs), when compared with either group I (5-FU) or II (magnetite alone; each group, $n = 7$; †, $P < 0.001$; *ns,* not significant).

References

1. Glehen O, Mohamed F, Gilly FN. Peritoneal carcinomatosis from digestive tract cancer: new management by cytoreductive surgery and intraperitoneal chemohyperthermia. Lancet Oncol 2004;5:219–28.
2. Kodera Y, Nakanishi H, Yamamura Y, et al. Prognostic value and clinical implications of disseminated cancer cells in the peritoneal cavity detected by reverse transcriptase-polymerase chain reaction and cytology. Int J Cancer 1998;79:429–33.
3. Sugarbaker PH, Yonemura Y. Clinical pathway for the management of resectable gastric cancer with peritoneal seeding: best palliation with a ray of hope for cure. Oncology 2000;58:96–107.
4. Nakanishi H, Kodera Y, Tatematsu M. Molecular method to quantitatively detect micrometastases and its clinical significance in gastrointestinal malignancies. Adv Clin Chem 2004;38:87–110.
5. Nakanishi H, Kodera Y, Yamamura Y, et al. Rapid quantitative detection of carcinoembryonic antigen-expressing free tumor cells in the peritoneal cavity of gastric-cancer patients with real-time RT-PCR on the lightcycler. Int J Cancer 2000;89:411–7.
6. Carmignani CP, Sugarbaker TA, Bromley CM, Sugarbaker PH. Intraperitoneal cancer dissemination: mechanisms of the patterns of spread. Cancer Metastasis Rev 2003;22:465–72.
7. Sakakura C, Hagiwara A, Shirasu M, et al. Polymerase chain reaction for detection of carcinoembryonic antigen-expressing tumor cells on milky spots of the greater omentum in gastric cancer patients: a pilot study. Int J Cancer 2001;95:286–9.
8. Naora H, Montell DJ. Ovarian cancer metastasis: integrating insights from disparate model organisms. Nat Rev Cancer 2005;5:355–66.
9. Munnell EW. The changing prognosis and treatment in cancer of the ovary. A report of 235 patients with primary ovarian carcinoma 1952–1961. Am J Obstet Gynecol 1968;100:790–805.
10. Piver MS. Ovarian carcinoma. A decade of progress. Cancer 1984;54:2706–15.
11. Tsujimoto H, Hagiwara A, Shimotsuma M, et al. Role of milky spots as selective implantation sites for malignant cells in peritoneal dissemination in mice. J Cancer Res Clin Oncol 1996;122:590–5.
12. Hagiwara A, Takahashi T, Sawai K, et al. Milky spots as the implantation site for malignant cells in peritoneal dissemination in mice. Cancer Res 1993;53:687–92.
13. Mochizuki Y, Nakanishi H, Kodera Y, et al. TNF-α promotes progression of peritoneal metastasis as demonstrated using a green fluorescence protein (GFP)-tagged human gastric cancer cell line. Clin Exp Metastasis 2004;21:39–47.
14. Krist LF, Kerremans M, Broekhuis-Fluitsma DM, Eestermans IL, Meyer S, Beelen RH. Milky spots in the greater omentum are predominant sites of local tumour cell proliferation and accumulation in the peritoneal cavity. Cancer Immunol Immunother 1998;47:205–12.
15. Krist LF, Koenen H, Calame W, et al. Ontogeny of milky spots in the human greater omentum: an immunochemical study. Anat Rec 1997;249:399–404.
16. Balkwill F, Mantovani A. Inflammation and cancer: back to Virchow? Lancet 2001;357:539–45.
17. Clevers H. At the crossroads of inflammation and cancer. Cell 2004;118:671–4.

18. Karin M, Cao Y, Greten FR, Li ZW. NF-κB in cancer: from innocent bystander to major culprit. Nat Rev Cancer 2002;2:301–10.

19. Greten FR, Eckmann L, Greten TF, et al. IKKβ links inflammation and tumorigenesis in a mouse model of colitis-associated cancer. Cell 2004;118:285–96.

20. Luo JL, Maeda S, Hsu LC, Yagita H, Karin M. Inhibition of NF-κB in cancer cells converts inflammation-induced tumor growth mediated by TNFα to TRAIL-mediated tumor regression. Cancer Cell 2004;6: 297–305.

21. Rosen H, Abribat T. The rise and rise of drug delivery. Nat Rev Drug Discov 2005;4:381–5.

22. Iinuma H, Maruyama K, Okinaga K, et al. Intracellular targeting therapy of cisplatin-encapsulated transferrin-polyethylene glycol liposome on peritoneal dissemination of gastric cancer. Int J Cancer 2002;99:130–7.

23. Allen TM. Ligand-targeted therapeutics in anticancer therapy. Nat Rev Cancer 2002;2:750–63.

24. Allen TM, Cullis PR. Drug delivery systems: entering the mainstream. Science 2004;303:1818–22.

25. Hagiwara A, Takahashi T, Kojima O, et al. Prophylaxis with carbon-adsorbed mitomycin against peritoneal recurrence of gastric cancer. Lancet 1992;339:629–31.

26. Rosen HR, Jatzko G, Repse S, et al. Adjuvant intraperitoneal chemotherapy with carbon-adsorbed mitomycin in patients with gastric cancer: results of a randomized multicenter trial of the Austrian Working Group for Surgical Oncology. J Clin Oncol 1998;16:2733–8.

27. Allum WH, Griffin SM, Watson A, Colin-Jones D. Guidelines for the management of oesophageal and gastric cancer. Gut 2002;50 Suppl 5:v1–23.

28. Studeny M, Marini FC, Dembinski JL, et al. Mesenchymal stem cells: potential precursors for tumor stroma and targeted-delivery vehicles for anticancer agents. J Natl Cancer Inst 2004;96:1593–603.

29. Studeny M, Marini FC, Champlin RE, Zompetta C, Fidler IJ, Andreeff M. Bone marrow-derived mesenchymal stem cells as vehicles for interferon-β delivery into tumors. Cancer Res 2002;62:3603–8.

30. Nakamizo A, Marini F, Amano T, et al. Human bone marrow-derived mesenchymal stem cells in the treatment of gliomas. Cancer Res 2005;65:3307–18.

31. Dullens HF, Rademakers LH, Doffemont M, Van Veen PT, Bulder R, Den Otter W. Involvement of the omental lymphoid organ in the induction of peritoneal immunity against tumor cells. Invasion Metastasis 1993;13:267–76.

32. Dullens HF, Rademakers LH, Cluistra S, et al. Parathymic lymph nodes during growth and rejection of intraperitoneally inoculated tumor cells. Invasion Metastasis 1991;11:216–26.

33. Burke B, Sumner S, Maitland N, Lewis CE. Macrophages in gene therapy: cellular delivery vehicles and *in vivo* targets. J Leukoc Biol 2002;72:417–28.

34. Burke B. Macrophages as novel cellular vehicles for gene therapy. Expert Opin Biol Ther 2003;3:919–24.

35. Ohashi N, Kodera Y, Nakanishi H, et al. Efficacy of intraperitoneal chemotherapy with paclitaxel targeting peritoneal micrometastasis as revealed by GFP-tagged human gastric cancer cell lines in nude mice. Int J Oncol 2005;27:637–44.

36. Shimizu Y, Yamakami K, Gomi T, et al. Protection against *Leishmania major* infection by oligomannose-coated liposomes. Bioorg Med Chem 2003;11:1191–5.

37. Shinkai M, Honda H, Kobayashi T. Preparation of fine magnetic particles and application for enzyme immobilization. Biocatalysis 1991;5:61–9.

38. Ikehara Y, Ikehara SK, Paulson JC. Negative regulation of T cell receptor signaling by Siglec-7 (p70/AIRM) and Siglec-9. J Biol Chem 2004;279:43117–25.

39. Roszkowski W, Szmigielski S, Janiak M, Wrembel JK, Roszkowski K, Hryniewicz W. Effect of hyperthermia on rabbit macrophages. Immunobiology 1980;157:122–31.

40. Yanase M, Shinkai M, Honda H, Wakabayashi T, Yoshida J, Kobayashi T. Intracellular hyperthermia for cancer using magnetite cationic liposomes: an *in vivo* study. Jpn J Cancer Res 1998;89:463–9.

41. Ito A, Shinkai M, Honda H, Kobayashi T. Heat-inducible TNF-α gene therapy combined with hyperthermia using magnetic nanoparticles as a novel tumor-targeted therapy. Cancer Gene Ther 2001;8: 649–54.

42. Ito A, Shinkai M, Honda H, Wakabayashi T, Yoshida J, Kobayashi T. Augmentation of MHC class I antigen presentation via heat shock protein expression by hyperthermia. Cancer Immunol Immunother 2001;50: 515–22.

43. Shinkai M, Yanase M, Suzuki M, et al. Intracellular hyperthermia for cancer using magnetite cationic liposomes. J Magnetism Magn Miner 1999;194:176–84.

44. Pollard JW. Tumour-educated macrophages promote tumour progression and metastasis. Nat Rev Cancer 2004;4:71–8.

45. Fidler IJ. The pathogenesis of cancer metastasis: the "seed and soil" hypothesis revisited. Nat Rev Cancer 2003;3:453–8.